A range estimation system using coded ultrasound

Riccardo Carotenuto

Dipartimento di Ingegneria dell'Informazione, delle Infrastrutture e dell'Energia Sostenibile

Università degli Studi "Mediterranea" di Reggio Calabria,

Loc. Feo di Vito, 89122 Reggio Calabria, Italy - +39 096 5169 3464 - r.carotenuto@unirc.it

Abstract

Touchless human-computer interfaces, augmented reality, and mixed reality, need the location of user's limbs or direction of sight in real time, which can be provided by accurate Real Time Locating Systems (RTLS). RTLS can be realized using wireless accurate positioning sensors and multilateration techniques that compute the location of sensors from distance estimates between them and a set of reference points. The main practical difficulty relies in estimating, within the required accuracy, the distances between the reference points and the remote sensors. In addition, the majority of modern applications require miniaturized sensors with both severe size and power supply constraints, and thus limited computational power. In this work, a distance estimation technique using coded ultrasound and a miniaturized sensor is proposed. A prototype of the distance estimation system has been realized and characterized. It is composed of a beacon that emits a coded ultra-acoustic signal, a central processing unit (CPU), and a wireless distance sensor. The main advantages of the proposed system are the high miniaturization and low power of the remote sensor.

Keywords: ultrasound ranging, coded ultrasound, wireless range sensor, correlation technique

Highlights

An accurate ranging system for touchless human-computer interfaces is proposed.

The system is composed by a central processing unit and a wireless remote sensor.

Coded ultrasound and cross-correlation are employed for accurate and noise robust ranging.

The computational load of the cross-correlation technique is moved from the remote sensors to the central processing unit thanks to a mirroring technique.

The reduced remote sensor functions allow minimal power supply and easy miniaturization.

For the final version see http://dx.doi.org/10.1016/j.sna.2015.12.006.

1. Introduction

Emerging technologies such as augmented reality, mixed reality, touchless interfaces, and domotics, necessitate accurate Real Time Locating Systems (RTLS). Among touchless interfaces, gestural interfaces are the most natural way to interact with machines, thanks to the ability to recognize and interpret movements of the human body. In the future, these interfaces will become more ubiquitous, due to their enormous impact in fields such as social life, work, health and entertainment. Touch-screens, accelerometer-equipped game pads, and smartphones available today are only a taste of this future. A gestural interface can be conveniently built using an RTLS equipped with a number of low-cost 3D wireless location sensors or tags. In addition, augmented reality requires knowing the direction of sight and the position of the user's head in respect to the observed scene for an accurate superimposition of synthetic information onto the real world. Glasses equipped with miniaturized position sensors can provide the required position and orientation information.

An accurate locating system with the capability of absolute object location with sufficient space and time resolution is a technology that has the potential of enabling a number of new applications in several fields of human life. Applications of man-machine gestural interfaces, interacting with virtual and augmented reality include domotics, controlling home appliances with human presence and movement; medical rehabilitation, monitoring body and limb location, posture and gesture; robotics, identifying objects and controlling flexible arms; security, controlling access, identifying persons, and monitoring assets. Further applications include safety, logistics, sport and military training, and gaming consoles.

Positioning techniques require carrying out distance measurements between reference points and a remote sensor. In the case of a simple 3D trilateration in a semi-space, at least three distance measurements are required to localize a remote sensor.

Current technologies on the market or in literature are not capable of providing ranging with sufficient time/space accuracy for implementing the described touchless interfaces or location-based applications at affordable cost.

Ultrasonic waves are commonly used to measure the distance between an emitter and a receiver. Ultrasonic distance measurement techniques include the time of flight (TOF) method, the single frequency continuous wave phase-shift analysis method, the combination of the TOF and phase-shift method, the multi-frequency continuous wave and phase-shift method, the multi-frequency amplitude-modulation (AM) method, the binary frequency shift-keyed (BFSK) method, several methods based on digital signal processing, e.g. cross-correlation methods, and many others [1-18].

In this work, a distance estimation technique based on coded ultrasound signals intended for implementing ranging systems with miniaturized sensors, is presented in detail in Section 3. Successively, a prototype of a system using the proposed distance estimation technique is described in Section 4. The experimental setup and some experimental results are presented in Section 5. The prototype is capable of estimating the range of a remote sensor with an accuracy of few millimeters within some meters, as required by most of the indoor applications.

2. Motivation

The methods [1-18] require synchronizing transmitter and receiver with an accuracy of few microseconds, a task that is very difficult to achieve when considering a wireless connection. However, with the aim of realizing a

For the final version see http://dx.doi.org/10.1016/j.sna.2015.12.006.

low cost system with minimal computational and power requirements, it would be desirable to employ a basic technique based on simple digital filtering and envelope detection.

An example of such a low cost method is found in [19]. The system is composed of a central unit and several remote sensors. The ranging is carried out emitting a short ultrasound pulse at a starting time and listening to the ultrasound pulse onboard the remote sensor. The incoming ultrasound signal is suitably transduced, conditioned, time sampled and digitally converted by the sensor circuitry. The sensor microprocessor continuously computes the incoming signal envelope. The maximum of the received pulse envelope at the microphone location is found and a proper timing signal is sent to the ranging system central unit in order to measure the time of flight. The expected ranging accuracy is roughly comparable to the pulse central wavelength.

Although on the market there are several microprocessors capable to carry out the computations required by the envelope-based technique within the given time constraints, they in turn require a power supply of several tens of milliwatts during operation, which is not compatible with a miniaturized battery. Massive processing and higher power levels are required by cross-correlation techniques. As a consequence, miniaturizing wireless range sensors results impossible even using the simplest techniques, and *a fortiori* employing more sophisticated techniques.

As a further obstacle, the envelope technique that could be potentially employed in conjunction with small ranging sensors, presents major issues on the range accuracy. In fact, ranging operations closely depend on the bandwidth and on the shape of the used ultrasound pulses. The wider is the bandwidth and the shorter is the ultrasound pulse, the better is the measurement accuracy. From this point of view, a desirable bandwidth should start from 20-25 kHz up to 200-300 kHz (e.g. $\lambda = 17.1$-1.1 mm in the range 20-300 kHz with speed of sound in air 343 m/s). However, the strong air adsorption and the unavailability of cost effective transducers for airborne ultrasound beyond 60-70 kHz limit the maximum ultrasound frequency below 60 kHz.

As a further issue, the detection of the time-of-arrival of a simple ultrasound pulse becomes very difficult or even impossible in presence of strong environmental acoustical noise. Moreover, multipath distortion, i.e. reflections on obstacles and successive additive/destructive interferences between multiple delayed copies of the same travelling wave, could distort the shape of the received pulses. In this scenario, techniques based on simple threshold detection, or even identification of the signal envelope maximum, could dramatically fail, showing relevant ranging errors up to several wavelengths λ (e.g. $\lambda = 6.9$ mm at 50 kHz and speed of sound in air 343 m/s).

The wireless return channel also adds timing uncertainty. Assuming the speed of sound in air about 343 m/s, and aiming to a ranging uncertainty of few millimeters, the time uncertainty must be kept below a few microseconds. Commercial RF transmitters for remote sensors (ISM band AM transmitters, ZigBee, Wi-Fi, etc.) were found not compliant with such requirement due to their communication protocol overhead.

3. The ranging technique and system architecture

In this section, an innovative solution to some of the above ranging issues is proposed. It exploits the advantages of the cross-correlation methods without charging the sensor of the related computational burden. The simple short ultrasound pulse of the previous envelope-detection method is replaced with a coded signal with improved autocorrelation, e.g. a linear up-chirp or a suitable Gold coded signal that show a well-peaked autocorrelation shape. The lag of the peak of the cross-correlation between the emitted and the received signals is proportional to

For the final version see http://dx.doi.org/10.1016/j.sna.2015.12.006.

the TOF.

The innovative idea is to avoid intensive cross-correlation computation in the sensor moving most of the computation to the central processing unit of the ranging system. This is achieved by employing a "mirroring" technique: a binary signal is derived from the ultrasound impinging on the remote sensor and continuously transmitted back to the CPU through a suitable return channel without any storage (see Figure 1). The binary signal must have autocorrelation properties similar to the ultrasonic one (see below). The maximum time uncertainty of the return channel is kept under a few microseconds in order to achieve the desired ranging accuracy. Thanks to the excellent autocorrelation property of the employed signals, the detection of the TOF is easily carried out by the CPU, even in case of strongly corrupted return signals. Differently from the envelope peak detection techniques, finding the cross-correlation peak allows for a distance estimation accuracy of the order of the current space sampling (i.e. the distance covered by the ultrasound between two consecutive time samples), which is in general much smaller than the ultrasound wavelength.

A drawback of all the TOF techniques is that the peak associated with the true delay is not always the highest peak. In some cases, in fact, the straight line path signal can be attenuated giving a lower peak than other signals coming from indirect multipaths. In other cases, a number of signals coming from indirect paths can combine to produce a peak higher than the one associated with the direct path signal. To prevent a misreading of the correct peak, a search mechanism can be applied to find the earliest arriving cross-correlation peak above the noise floor [20].

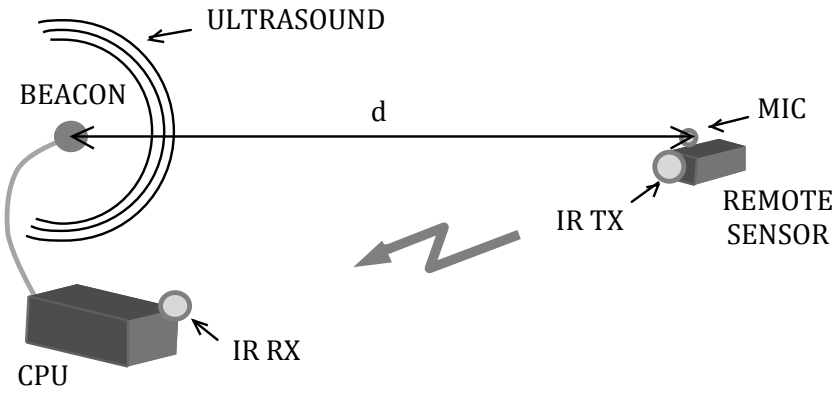

Figure 1. System Architecture: the beacon emits ultrasound chirps and the impinged remote sensor sends back IR signals to the radio base CPU, where a cross-correlation based algorithm estimates the range *d* of the sensor.

The binary signal sent through the return channel, here called "modified binary signal" (MBS), is derived from the incoming chirp signal by generating a short pulse at each zero-crossing transition from low to high of the original signal. This is carried out by a simple analog circuitry. The actual duration of each short pulse depends on the specific technology used for the return channel, as detailed below. The MBS can be very easily processed and transmitted over any digital channel, and it shows a very sharp autocorrelation peak. In Figure 2, a chirp and its derived MBS are showed (left) and their autocorrelations compared (right). It is worth noting that the MBS shows a sharper autocorrelation peak compared to that computed starting from the original chirp. The triangular shape of the MBS autocorrelation, which could interfere with correct peak detection, can be cancelled by

For the final version see http://dx.doi.org/10.1016/j.sna.2015.12.006.

subtracting the mean value from the signal.

In details, the sensor circuitry amplifies, filters and squares the signal received by the onboard microphone. Then it transmits a short pulse to the CPU at each zero-to-one transition of the squared signal through the RF, or infra-red (IR), return channel, i.e. one bit per transition.

The CPU receives and time samples the MBS, then computes the cross-correlation between the received signals and a copy of the expected signal, previously stored in the CPU memory after a suitable calibration procedure. This calibration is carried out only once, after the initial system setup, to compensate for system delay and signal distortion along the whole chain. The position of the peak in the computed cross-correlation vector is proportional to the time-of-flight of the ultrasound signal travelling from the emitter to the remote sensor, provided that the return channel time delay is constant and known.

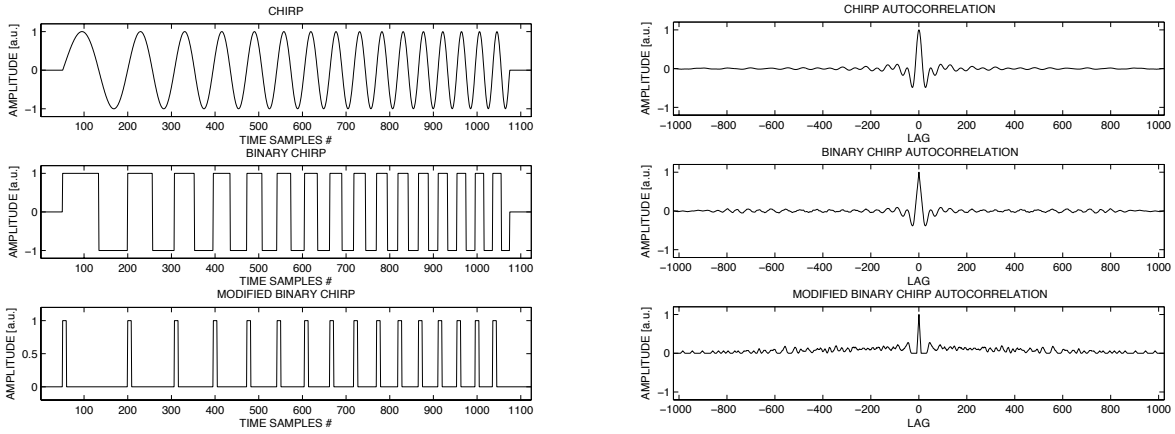

Figure 2. Examples of short chirp, binary chirp, modified binary chirp (left), and their autocorrelations (right).

This range estimation process is summarized in the following system functional diagram, where the one direction return channel can be realized using different technologies, including several RF and IR techniques (OOK, CDMA, etc.). Here it is realized using a LED as transmitter and the RX section of a commercial OOK IR transceiver (see Fig. 3).

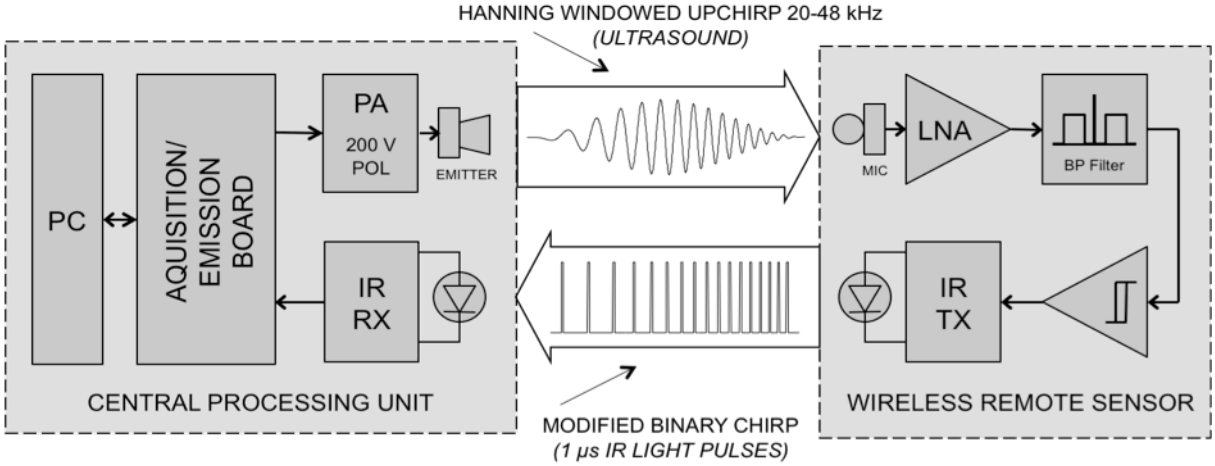

Figure 3. Ultrasound ranging system functional diagram: CPU (left), ultrasound and return IR signals (center), and wireless remote range sensor (right).

For the final version see http://dx.doi.org/10.1016/j.sna.2015.12.006.

The proposed operating scheme shows remarkable advantages: most of the computation effort required to accurately find the arrival time of the ultrasound signals is moved from the remote sensor to the CPU, since the cross-correlation computation is carried out entirely by the CPU. In this way, the remote sensor circuitry and its power consumption are dramatically reduced. Coding provides good noise immunity both to the ultrasound and to the return channel. If needed, different codes can be assigned to different ultrasound emitters, and to different sensors, using return channels with suitable code.

4. Hardware design

4.1 System design choices

The prototype has been built with the specific aim of demonstrating the effectiveness of the proposed technique using only off-the-shelf components as ultrasound emitters and microphones. In fact, the use of ready and mature technologies is very important for a ranging system intended to become a widely used human-machine interface with very low mass-production costs.

A linear up-chirp in the bandwidth 20-48 kHz is employed. In order to use commercial components, the chirp frequency bandwidth has been chosen just beyond the upper frequency of the working bandwidth of commercial high quality microphones, from 20 kHz up to 48 kHz, while the sampling frequency was set at 192 kSamples/s. At this sampling frequency and assuming the speed of sound in air 343 m/s, each time sample represents a space interval of about 1.8 mm, which actually sets the limit of the range estimation accuracy of the system. In the present experimental setup, the chirp signal emitted by the beacons is composed of 1024 samples at 192 kSamples/s. The emitted signal is Hanning windowed to avoid audible “clicking”. An increased duration of the chirp improves the SNR of the system, but at the expenses of both ranging rate and CPU computational effort. The components of the prototype are listed below.

4.2 CPU

A PC is employed as the processing unit of the system. Algorithms written in MATLAB (The MathWorks™, Natick, MA, USA) are executed on the PC in order to build the acoustic signals that are emitted by the transducers, and to acquire, store and analyze the return signals received from the remote sensor.

Signals are emitted and acquired by the MOTU 828 mk3 board (MOTU, Cambridge, MA, USA). This board provides ten analog inputs and ten analog outputs that can operate at a sample rate up to 192 kSamples/s. However, the present prototype uses only one output and one input. The connection with the PC is realized via FireWire. The main feature of the MOTU board is the capability to maintain sample-level synchronicity between emitted and recorded sequences, which is essential for a correct TOF measurement.

4.3 Ultrasound emitter

As ultrasound emitter, the Series 7000 Electrostatic Transducer (SensComp Inc., Livonia, MI, USA) was employed. Preliminarily tests have shown that this specific model is able to emit sufficiently accurate chirp signals in the desired ultra-acoustic band. Furthermore, such a transducer is small sized and has a small acoustic output emission window (diameter 20 mm), which guarantees a sufficiently wide emission lobe. The shape of its emission lobe varies considerably according to the frequency of the emission. In the frequency range of interest, the narrowest emission cone aperture (i.e. the worst case) is about 60°. This could potentially lead to a spatial coverage problem if the emitter is not properly placed according to the space region to be insonified. Also the

For the final version see http://dx.doi.org/10.1016/j.sna.2015.12.006.

emission diagram shows notches whose angular positions depend on the emitted frequency. Using more than one transducer per beacon allows covering wider solid angles, when required. Properly shaping a custom horn-loaded emitter could help in widening the emission cone. This issue will be investigated in the near future. Notches in the emission band or in the emission diagram are seen as disturbances by the decode processing at CPU.

The transducer also has a reasonable low cost for mass production. The electrostatic technology requires high voltage bias and driving signal. For these reasons, the electrostatic transducers are driven by a specific additional transformer circuitry.

4.4 Transducer driver

The output power amplifier and biasing box hosts a power amplifier and a bias circuit driving the electrostatic transducer. The signal voltage elevator is realized using miniaturized 1:100 coil transformer LPR6235-752S (Coilcraft, Glasgow, UK), while a 200 V DC bias voltage is obtained employing one ultra-miniature DC to HV DC Converter Q02-5-R (EMCO High Voltage Corporation, Sutter Creek, CA, USA).

With a chirp maximum frequency of 48 kHz, there is a maximum of $24 \cdot 10^3$ transitions per second, and the required maximum digital transfer rate is 24 kbit/s, which is the minimum return channel bandwidth required by a single sensor. The infrared receiver is realized using the RX section of the OOK transceiver TFDU6101E (Vishay Semiconductors, Pennsylvania, USA), which works at the wavelength of 870 nm with a transfer rate of up to 4 Mbit/s.

4.5 Remote sensor

The remote sensor (see Fig. 4) includes a miniature microphone FG-6163 (Knowles Acoustics, Itasca, Illinois, USA), which is a micromachined condenser microphone in a cylindrical shape package, length and diameter 2.6 mm, acoustical receiver window diameter 0.79 mm, and weight 80 mg. The receiving acoustical window, which is small in respect of the used wavelength range (about 7.1-17.1 mm in the 20-48 kHz range, with sound speed in air 343 m/s), ensures a good approximation of a point-like omnidirectional receiver. Moreover, a very small microphone is an advantage for the intended applications. In fact, the remote sensor, as a whole, must be sufficiently small and lightweight to be easily worn by people.

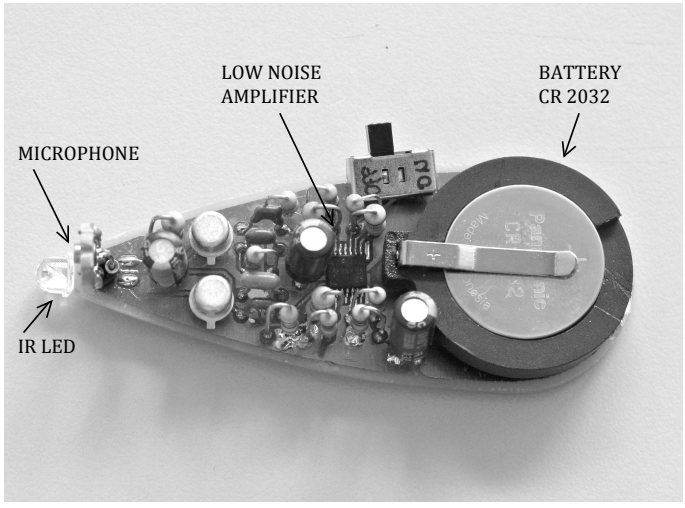

Figure 4. Picture of the prototype remote sensor, including miniaturized capacitive microphone, signal conditioning, IR transmission section, and standard button type CR2032 lithium battery.

For the final version see http://dx.doi.org/10.1016/j.sna.2015.12.006.

The microphone is conditioned by a low-power circuitry including low noise pre-amplification and amplification stages (TLV2464, Texas Instruments, Texas, USA), a 20-48 kHz band-pass filter, and a Schmitt trigger in order to square the received signal and to drive, through a BJT power amplifier, an IR LED TSFF5510 (Vishay Semiconductors, Pennsylvania, USA), according to the adopted on-off-keying amplitude modulation scheme. Finally, the remote sensor circuitry is powered by a standard button lithium battery type CR2032.

5. Experimental results

5.1 Processing chain evaluation

During each ranging operation, the beacon emits a linear up-chirp from 20 to 48 kHz, at predefined time intervals. The ultrasound signal received by the remote sensor is amplified, squared and modified in order to transmit back to the CPU the low-to-high transitions only, as a single asynchronous and short duration "1" bit. The signal received by the IR RX is recorded by the acquisition board MOTU at 192 kSamples/s and then processed with a suitable MATLAB code on the PC. The listening window was set to 900 samples, whose duration is 4.7 ms at 192 kSamples/s and equivalent to a range of about 1.6 meters, assuming a speed of sound in air of 343 m/s.

In Figure 5, the zoomed initial portion of the experimental chirp received, filtered and amplified by the wireless sensor circuitry (top) and of the modified binary chirp recorded from the IR RX after reception through the return channel as provided to the MOTU input channel (bottom), are shown. The relatively long duration of the pulses in Figure 5 (bottom) depends on the employed IR transceiver.

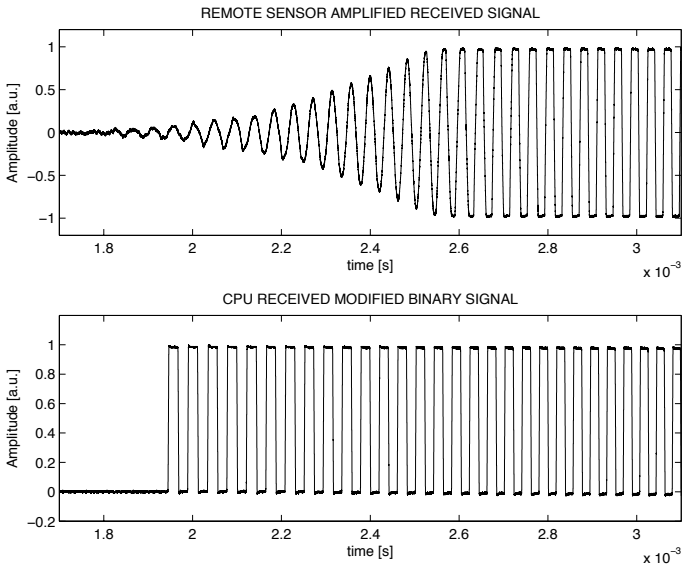

Figure 5. Example zoomed portions of the experimental chirp, received, filtered and amplified by the wireless sensor circuitry (top), and of the modified binary chirp recorded from the IR RX after reception through the return channel (bottom), with high SNR. The emitted signal is Hanning windowed to avoid audible "clicking".

The data displayed in Figure 5 were obtained with a sufficiently high SNR to clearly show the processing chain behavior, while during regular operation, in presence of reasonable acoustical noise, the received modified binary signal shows a significant number of uncorrelated commutations (see below). The recorded binary signal

For the final version see http://dx.doi.org/10.1016/j.sna.2015.12.006.

is cross-correlated with a stored version of the modified binary chirp, acquired through the calibration procedure already explained in the previous section.

The actual TOF is obtained after a second calibration step, by comparing the measured distance between the beacon and the microphone with the computed one in order to compensate for the internal constant system processing delays. This procedure is required at the first use of the system only.

During the experiments, the sound velocity was assumed to be constant at 343 m/s. The variation of sound velocity due to temperature and humidity were assumed to be negligible as the measurements were taken over a short period of time (e.g. when the temperature increases from 20 °C to 21 °C, the sound speed varies less than 0.2%).

5.2 Precision and reliability considerations

The lower bound for the time accuracy detection of the time delay is given by the Cramér-Rao formulation [21]:

$$\sigma_D^2 \geq \frac{1}{16\pi^2 BTf_0^2 SNR}, \tag{1}$$

where BT is time-bandwidth product, f_0 is the center frequency and SNR is the signal-to-noise ratio (SNR high enough to have no ambiguity in the peak detection).

In the present case, B = 25 kHz, T = 5.3 ms, f_0 = 32.5 kHz, SNR = 20 dB, and $\sigma_D^2 \geq 2.25 \cdot 10^{-16}$ s. Assuming the sound velocity 343 m/s at 20 °C, the distance error lower bound results about 16 μm. However, we previously mentioned that the MOTU board digitizes the input signal at a rate of 192 kSamples/s. The time precision of the system is limited by its sampling rate and cannot be shorter than the duration of one sample. The highest available range precision is therefore given by $p = vT_s$, where p is the precision margin in meters, v the velocity of sound and T_s the time between two successive samples.

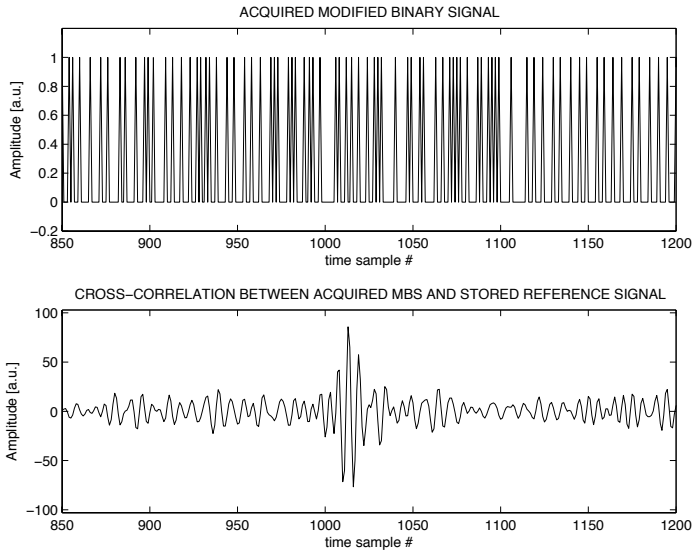

Figure 6. Zoomed portion of the experimental acquired modified binary signal (top) and its cross-correlation with the expected modified binary signal (bottom). The position of the cross-correlation peak is still well recognizable with a 25 dB SNR.

For the final version see http://dx.doi.org/10.1016/j.sna.2015.12.006.

At 20 °C, this margin is equivalent to about 1.8 mm. In addition, signal loss and noise can cause the system to generate unreliable ranging data. Possibly wrong cross-correlation peak lag recognition due to temporary strong acoustical disturbances, and alterations in the sound speed due to humidity, temperature and air mass flow are other major limiting causes. Figure 6 shows the zoomed portion of the experimental acquired modified binary chirp (top) and its cross-correlation with the expected modified binary chirp (bottom) with a 25 dB SNR. In order to cancel the triangular-shaped waveform of the unipolar signals cross-correlation, and consequently to easy the peak detection, the mean value was subtracted from the expected MBS before cross-correlation. The position of the cross-correlation peak results well recognizable.

5.3 Experimental ranging results

The experimental ranging results and their standard deviations when the remote sensor is moved along a straight line are shown in Figure 7. The measurements are taken at steps of 4 cm along a straight line of length 1 m. The line path starts from a point placed on the emitter axis at 50 cm from it and goes up to a distance of 135 cm from the emitter, from the axis of the emission cone to its periphery. It shows a 45° angle in respect to the emitter axis and it is well insonified by the 60° emission cone of the emitter.

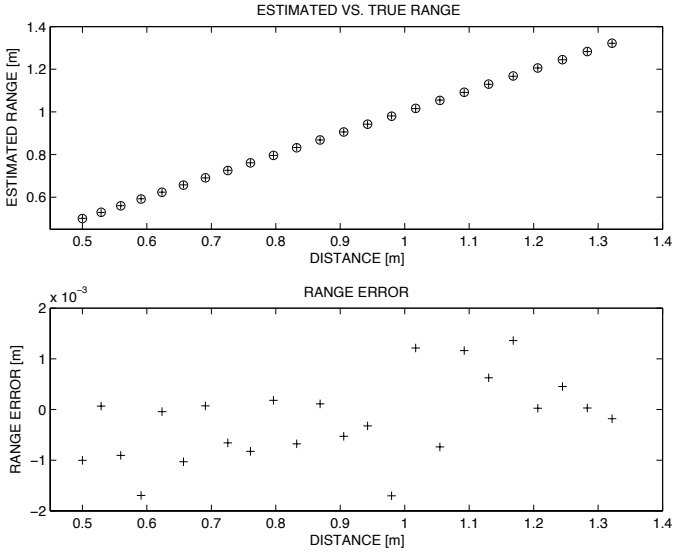

Figure 7. Experimental ranging results (cross) compared to true distances (circle) (top). Range error (bottom).

For the final version see http://dx.doi.org/10.1016/j.sna.2015.12.006.

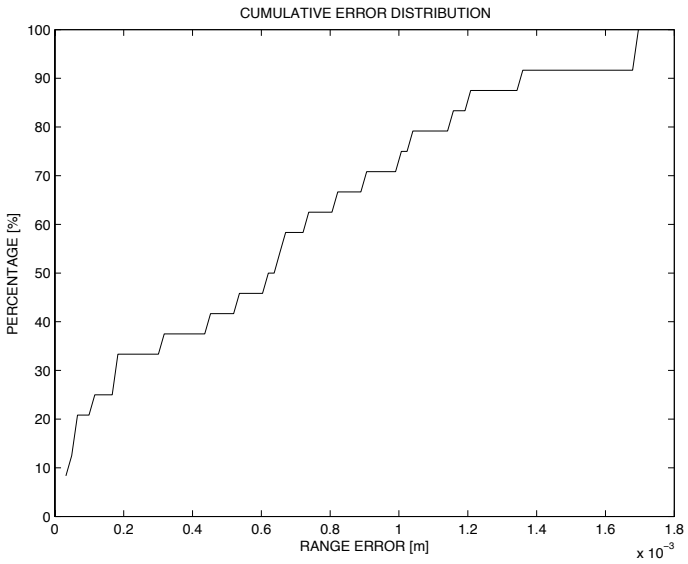

Figure 8. Cumulative error distribution of the estimated range using cross-correlation (percent of readings with error less than abscissa).

In order to be able to detect faulty measurements in the experiments and to evaluate the reliability of the proposed technique, each measurement was repeated 250 times. As a result, no abnormalities were measured and no outliers were eliminated. In consideration of the foreseen real-time use of the ranging system, where it is unpractical to average multiple measurements, in Figure 7 the experimental results of a single ranging operation are plotted. The estimated ranges are in good agreement with the ones measured using the reference mechanical means. The absolute error is limited to ±1.8 mm, as expected.

In Figure 8, the cumulative error distribution of the estimated range using cross-correlation is shown, according to the range quantization of ±1.8 mm of the system.

During operation, the measured average current provided by the sensor onboard button lithium battery type CR2032 was about 8 mA, mainly adsorbed by the IR LED.

6. Conclusions

A distance estimation technique using coded ultrasound has been proposed and demonstrated. The proposed technique relies on a cross-correlation technique, which provides distance estimation accuracy in the order of the space-sampling interval, much smaller than the employed ultrasound wavelength, showing a good robustness against disturbances. Reasonably low ultrasound frequencies have been used, allowing the use of off-the-shelf and low cost components, still obtaining millimeters ranging accuracy. The major drawback of any cross-correlation technique is that it requires intensive on-board computation, which cannot be executed on-board by a miniaturized battery-operated remote sensor. In the proposed system, this issue has been solved by moving all the digital processing from the remote sensor to the CPU. The prototype shows ranging accuracy of about ±1.8 mm within a range of 1.35 m from the emitter. Ranging and display MATLAB codes run on a standard PC notebook. One of the main advantages of the proposed technique is that it potentially allows the

For the final version see http://dx.doi.org/10.1016/j.sna.2015.12.006.

realization of miniaturized system-on-chip location sensors, whilst maintaining satisfactory ranging accuracy and robustness against noise.

Very promising applications of the ranging method proposed here include but are not limited to gestural interfaces, domotics, real time mapping of human body movements, and gaming interfaces. New coding schemes and processing algorithms will be investigated in the near future.

Acknowledgments

The author wishes to thank in particular Dr. P. Tripodi, who has helped to realize the system hardware described in this work. The author gratefully acknowledges the support of the European Commission under the Marie Curie Transfer of Knowledge (TOK) Program (contract no. MTKD-CT-2006-042269), and the support of Pentasonics S.r.l., Rome, Italy.

References

[1] F. Aldawi, A. P. Longstaff, S. Fletcher, P. Mather and A. Myers, A high accuracy ultrasound distance measurement system using binary frequency shift-keyed signal and phase detection, Proc. Computing and Engineering Annual Researchers' Conference 2007, Univ. Huddersfield, Huddersfield, (2007) 1-7.

[2] A. Hernández, J. Ureña, J.J. García, M. Mazo, D. Hernanz, J. Dérutin, and J. Sérot, Ultrasonic ranging sensor using simultaneous emissions from different transducers, IEEE Trans. Ultrason. Ferroelect. Freq. Contr., 51 (2004) 1660-1670.

[3] Y. P. Huang, J. S. Wang, K. N. Huang, C. T. Ho, J. D. Huang, and M. S. Young, Envelope pulsed ultrasonic distance measurement system based upon amplitude modulation and phase modulation, Rev. Sci. Instrum., 78 (2007), 65103 - 65103-8.

[4] P. Zhang, H. Guo, High-precision ultrasonic ranging system, Electronic Measurement & Instruments (ICEMI), 2011 10th International Conference on, 2 (2011) 47-50.

[5] X. Zhao, Q. Luo, B. Han, X. Li, A novel ultrasonic ranging system based on the self-correlation of pseudo-random sequence, Information and Automation 2009, ICIA '09, Intl. Conf. on, (2009) 1124-1128.

[6] T. Chia-Chang, J.F. Figueroa, E. Barbieri, A method for short or long range time-of-flight measurements using phase-detection with an analog circuit, IEEE Trans. Instrum. Meas., 50 (2001) 1324-1328.

[7] A.M. Sabatini, A. Rocchi, Sampled baseband correlators for in-air ultrasonic rangefinders, IEEE Trans. Ind. Electron., 45 (1998) 341-350.

[8] A.M. Sabatini, A stochastic model of the time-of-flight noise in airborne sonar ranging systems, IEEE Trans. Ultrason. Ferroelect., Freq. Contr., 44 (1997) 606-614.

[9] A.M. Sabatini, Correlation receivers using Laguerre filter banks for modelling narrowband ultrasonic echoes and estimating their time-of-flights, IEEE Trans. Ultrason. Ferroelect. Freq. Contr., 44 (1997) 1253-1263.

[10] K. Audenaert, H. Peremans, Y. Kawahara, J. Van Campenhout, Accurate ranging of multiple objects using ultrasonic sensors, Robotics and Automation, 1992. Proceedings, 1992 IEEE Intl. Conf., 2 (1992) 1733-1738.

[11] M.M. Saad, C.J. Bleakley, S. Dobson, Robust High-Accuracy Ultrasonic Range Measurement System, IEEE Trans. Instrum. Meas., 60 (2011) 3334-3341.

[12] C. Wan-Jie, C. Fan-Ren, A novel ranging method by code and multiple carriers of FHSS systems, Wireless Telecommunications Symposium (WTS), (2012) 1-6.

[13] K. Nakahira, S. Okuma, T. Kodama, T. Furuhashi, The use of binary coded frequency shift keyed signals for multiple user sonar ranging, Networking, 2004 IEEE Intl. Conf. Sensing and Control, 2 (2004) 1271-1275.

[14] S. Huang, C. Huang, K. Huang, M. Young, A high accuracy ultrasonic distance measurement system using binary frequency shift- keyed signal and phase detection, Rev. Sci. Instrum., 73 (2002) 3671.

[15] Y. Huang and M. Young, An Accurate Ultrasonic Distance Measurement System with Self Temperature Compensation, Instrum. Sci. Tech., 37 (2009) 124-133.

[16] B. Barshan, Fast processing techniques for accurate ultrasonic range measurements, Meas. Sci. Tech., 11 (2000) 45-50.

For the final version see http://dx.doi.org/10.1016/j.sna.2015.12.006.

[17] D. Marioli, C. Narduzzi, C. Offelli, D. Petri, E. Sardini, A. Taroni, Digital time-of-flight measurement for ultrasonic sensors, IEEE Trans. Instrum. Meas., 41 (1992) 93-97.
[18] J. Gonzalez, C. J. Bleakley, Accuracy of spread spectrum techniques for ultrasonic indoor location, Digital Signal Processing, 2007 15th Intl Conf., (2007) 284-287.
[19] R. Ionescu, R. Carotenuto, F. Urbani, 3D localization and tracking of objects using miniature microphones, Wireless Sensor Network, 3 (2011) 147-157.
[20] L. Girod, D. Estrin, Robust range estimation using acoustic and multimodal sensing, Proc. IEEE/RSJ Intl. Conf. Intelligent Robots and Systems IROS 2001, (2001).
[21] A.J. Weiss, E. Weinstein, Fundamental limitations in passive time delay estimation-Part I: Narrow-band systems, IEEE Trans. Acoust. Speech Signal Process., 31 (1983) 472-486.

For the final version see http://dx.doi.org/10.1016/j.sna.2015.12.006.